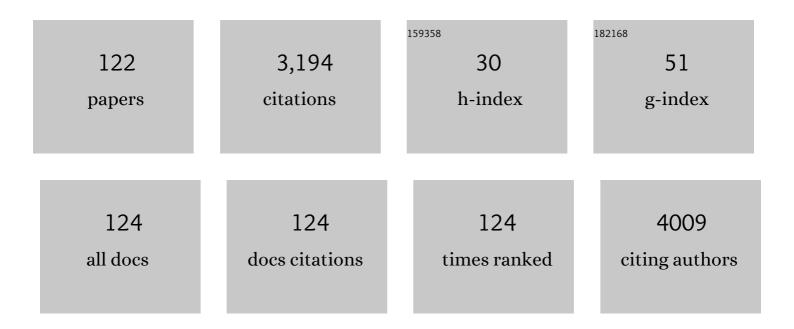
Xiaoyang Liu

List of Publications by Year in descending order

Source: https://exaly.com/author-pdf/807936/publications.pdf Version: 2024-02-01



#	Article	IF	CITATIONS
1	Carbon-Coated Rice Husk-Derived SiO2/C Composites As Anodes for Lithium-Ion Batteries: Comparison between CTEP and PVC Carbon Coatings. Journal of Electronic Materials, 2022, 51, 68-76.	1.0	3
2	Core–shell structured C/SiO2 composites derived from Si-rich biomass as anode materials for lithium-ion batteries. Ionics, 2022, 28, 151-160.	1.2	6
3	The direct growth of Mn _{0.6} Ni _{0.4} CO ₃ nanosheet assemblies on Ni foam for high-performance supercapacitor electrodes. New Journal of Chemistry, 2022, 46, 2635-2640.	1.4	1
4	Preparation of nickel-bound porous carbon and its application in supercapacitors. Inorganic Chemistry Frontiers, 2022, 9, 652-661.	3.0	4
5	Design of NiCo ₂ O ₄ @NiMoO ₄ core–shell nanoarrays on nickel foam to explore the application in both energy storage and electrocatalysis. Materials Chemistry Frontiers, 2022, 6, 1056-1067.	3.2	11
6	NiCo2S4@MoS2 core/shell nanorod arrays for fabrication of high-performance asymmetric supercapacitors with high mass loading. Journal of Energy Storage, 2022, 51, 104518.	3.9	8
7	PVC Coated Lignin/silica Composites Derived from Biomass Rice Husks as a High Performance Anode Material for Lithium Ion Batteries. ChemistrySelect, 2022, 7, .	0.7	0
8	Hierarchical copper cobalt sulfide nanobelt arrays for high performance asymmetric supercapacitors. Inorganic Chemistry Frontiers, 2021, 8, 3025-3036.	3.0	30
9	Facile Synthesis of MgCo ₂ O ₄ @MMoO ₄ (M = Co, Ni) Nanosheet Arrays on Nickel Foam as an Advanced Electrode for Asymmetric Supercapacitors. Energy & Fuels, 2021, 35, 6272-6281.	2.5	7
10	Facile preparation of hydrogenated graphene by hydrothermal methods and the investigation of its ferromagnetism. Chinese Chemical Letters, 2021, 32, 3596-3600.	4.8	7
11	Extracting lignin-SiO2 composites from Si-rich biomass to prepare Si/C anode materials for lithium ions batteries. Materials Chemistry and Physics, 2021, 262, 124331.	2.0	13
12	One-step fabrication of few-layer g-C3N4 by pressure quenching and investigation of its exfoliating effect. Chemical Engineering Science, 2021, 233, 116395.	1.9	4
13	Acid Hydrolysis to Provide the Potential for Rice-Husk-Derived C/SiO2 Composites for Lithium-Ion Batteries. Journal of Electronic Materials, 2021, 50, 4426-4432.	1.0	3
14	Facilely synthesized N-doped graphene sheets and its ferromagnetic origin. Chinese Chemical Letters, 2021, 32, 3841-3846.	4.8	9
15	Microwaveâ€Assisted Rapid Synthesis of Urchinâ€Like Bimetallic Mn–Co Carbonate Composites for Highâ€Performance Supercapacitors. ChemistrySelect, 2021, 6, 5633-5639.	0.7	0
16	Synthesis of core-shell structured Ni3S2@MnMoO4 nanosheet arrays on Ni foam for asymmetric supercapacitors with superior performance. Journal of Alloys and Compounds, 2021, 874, 159860.	2.8	20
17	Controllable Synthesis and Luminescence Properties of Zn 2 GeO 4  : Mn 2+ Nanorod Phosphors. ChemistrySelect, 2021, 6, 10554-10560.	0.7	9
18	Fabrication of Phosphorus-Doped Cobalt Silicate with Improved Electrochemical Properties. Molecules, 2021, 26, 6240.	1.7	3

#	Article	IF	CITATIONS
19	NiWO ₄ Microflowers on Multi-Walled Carbon Nanotubes for High-Performance NH ₃ Detection. ACS Applied Materials & Interfaces, 2021, 13, 52850-52860.	4.0	61
20	Synthesis of hierarchical Ni3S2@NiMoO4 core-shell nanosheet arrays on Ni foam for high-performance asymmetric supercapacitors. Journal of Energy Storage, 2021, 44, 103459.	3.9	14
21	Synthesis of few-layer N-doped graphene from expandable graphite with melamine and its application in supercapacitors. Chinese Chemical Letters, 2020, 31, 559-564.	4.8	17
22	A Highly Sensitive and Stable SERS Sensor for Malachite Green Detection Based on Ag Nanoparticles In Situ Generated on 3D MoS ₂ Nanoflowers. ChemistrySelect, 2020, 5, 354-359.	0.7	15
23	Self-assembled lignin-silica hybrid material derived from rice husks as the sustainable reinforcing fillers for natural rubber. International Journal of Biological Macromolecules, 2020, 145, 410-416.	3.6	38
24	High pressure: a feasible tool for the synthesis of unprecedented inorganic compounds. Inorganic Chemistry Frontiers, 2020, 7, 2890-2908.	3.0	18
25	Nanotwinned Structure-Dependent Photocatalytic Performances of the Multipod Frameworks of Cu7S4 Hollow Microcages. Frontiers in Chemistry, 2020, 8, 15.	1.8	6
26	Interfacial self-propagation of oleophilic vaterite in crude oil emulsion and its application for reinforcing polyethylene. Powder Technology, 2020, 363, 642-651.	2.1	4
27	Preparation of a graphene–phosphorene composite by pressure quenching and its ferromagnetism. Chemical Communications, 2020, 56, 2016-2019.	2.2	6
28	Facile Synthesis of Hierarchical MgCo ₂ O ₄ @MnO ₂ Core-Shell Nanosheet Arrays on Nickel Foam as an Advanced Electrode for Asymmetric Supercapacitors. Journal of the Electrochemical Society, 2020, 167, 020510.	1.3	13
29	A high-performance electrode based on the ZnCo2O4@CoMoO4 core-shell nanosheet arrays on nickel foam and their application in battery-supercapacitor hybrid device. Electrochimica Acta, 2020, 347, 136278.	2.6	35
30	Self-template synthesis of nitrogen-doped porous carbon derived from rice husks for the fabrication of high volumetric performance supercapacitors. Journal of Energy Storage, 2020, 30, 101405.	3.9	53
31	Controllable synthesis of cobalt molybdate nanoarrays on nickel foam as the advanced electrodes of alkaline battery-supercapacitor hybrid devices. Journal of Alloys and Compounds, 2020, 835, 155244.	2.8	19
32	Selfâ€healing behaviors of sulfobetaine polyacrylamide/chromium gel decided by viscosity and chemical compositions. Journal of Applied Polymer Science, 2019, 136, 46991.	1.3	1
33	Coal Tar Electrode Pitch Modified Rice Husk Ash as Anode for Lithium Ion Batteries. Journal of the Electrochemical Society, 2019, 166, A2425-A2430.	1.3	13
34	Fabrication of CuO@NiMoO4 core-shell nanowire arrays on copper foam and their application in high-performance all-solid-state asymmetric supercapacitors. Journal of Power Sources, 2019, 440, 227164.	4.0	30
35	Potential impact of organic ligands on the antibacterial activity of silver nanoparticles. New Journal of Chemistry, 2019, 43, 2870-2874.	1.4	9
36	The Microwaveâ€Assisted Hydrothermal Synthesis of CoV ₂ O ₆ and Co ₃ V ₂ O ₈ with Morphology Tuning by pH Adjustments for Supercapacitor Applications. ChemistrySelect, 2019, 4, 956-962.	0.7	24

#	Article	IF	CITATIONS
37	A surfactantâ€free synthesis of the silica nanosphereâ€supported ultrafine silver nanoparticles and their antibacterial effects. Journal of the Chinese Chemical Society, 2019, 66, 815-821.	0.8	3
38	Microwave-assisted green synthesis of manganese molybdate nanorods for high-performance supercapacitor. Ionics, 2019, 25, 4361-4370.	1.2	12
39	Enhanced Antibacterial Activity of Poly (dimethylsiloxane) Membranes by Incorporating SiO2 Microspheres Generated Silver Nanoparticles. Nanomaterials, 2019, 9, 705.	1.9	15
40	Synthesis of ZnFe 2 O 4 @MnO 2 Multilevel Nanosheets Structure and Its Electrochemical Properties as Positive Electrodes for Asymmetric Supercapacitors. ChemistrySelect, 2019, 4, 5168-5177.	0.7	5
41	The template effect of silica in rice husk for efficient synthesis of the activated carbon based electrode material. Journal of Alloys and Compounds, 2019, 789, 777-784.	2.8	35
42	Facile synthesis of mesoporous ZnCo2O4 nanowire arrays and nanosheet arrays directly grown on nickel foam for high-performance supercapacitors. Inorganic Chemistry Communication, 2019, 101, 16-22.	1.8	17
43	One-step electrodeposition fabrication of Ni3S2 nanosheet arrays on Ni foam as an advanced electrode for asymmetric supercapacitors. Science China Materials, 2019, 62, 699-710.	3.5	60
44	A novel polyhedron-based metal–organic framework with high performance for gas uptake and light hydrocarbon separation. Dalton Transactions, 2018, 47, 5005-5010.	1.6	17
45	A facile one-step hydrothermal approach to synthesize hierarchical core–shell NiFe ₂ O ₄ @NiFe ₂ O ₄ nanosheet arrays on Ni foam with large specific capacitance for supercapacitors. RSC Advances, 2018, 8, 15222-15228.	1.7	40
46	Acetic Acid Assistant Hydrogenation of Graphene Sheets with Ferromagnetism. Chemical Research in Chinese Universities, 2018, 34, 344-349.	1.3	8
47	Fabrication of the porous MnCo2O4 nanorod arrays on Ni foam as an advanced electrode for asymmetric supercapacitors. Acta Materialia, 2018, 152, 162-174.	3.8	95
48	The synthesis of hierarchical ZnCo ₂ O ₄ @MnO ₂ core–shell nanosheet arrays on Ni foam for high-performance all-solid-state asymmetric supercapacitors. Inorganic Chemistry Frontiers, 2018, 5, 597-604.	3.0	58
49	Hierarchical 3D NiFe ₂ O ₄ @MnO ₂ core–shell nanosheet arrays on Ni foam for high-performance asymmetric supercapacitors. Dalton Transactions, 2018, 47, 2266-2273.	1.6	60
50	Preparation of Fluorescent Thiol Groupâ€Functionalized Silica Microspheres for the Detection and Removal of Silver Ions in Aqueous Solutions. Journal of the Chinese Chemical Society, 2018, 65, 591-596.	0.8	9
51	Pressure quenching: a new route for the synthesis of black phosphorus. Inorganic Chemistry Frontiers, 2018, 5, 669-674.	3.0	17
52	A novel crystal-modified electrode based on polyoxometalate (Bu4N)4PW11O39FeIII (H2O) for electrocatalysis. Journal of Solid State Electrochemistry, 2018, 22, 237-243.	1.2	9
53	Two types of B-site ordered structures of the double perovskite Y2CrMnO6: experimental identification and first-principles study. Inorganic Chemistry Frontiers, 2018, 5, 217-224.	3.0	4
54	Fabrication of porous ZnCo2O4 nanoribbon arrays on nickel foam for high-performance supercapacitors and lithium-ion batteries. Electrochimica Acta, 2018, 260, 823-829.	2.6	55

#	Article	IF	CITATIONS
55	Fabrication of hierarchical MnMoO4·H2O@MnO2 core-shell nanosheet arrays on nickel foam as an advanced electrode for asymmetric supercapacitors. Chemical Engineering Journal, 2018, 334, 1466-1476.	6.6	121
56	Surfactantâ€Free In Situ Synthesis of Subâ€5 nm Silver Nanoparticles Embedded Silica Subâ€Microspheres as Highly Efficient and Recyclable Catalysts. ChemistrySelect, 2018, 3, 10352-10356.	[°] 0.7	3
57	SiO ₂ /C Composite Derived from Rice Husks with Enhanced Capacity as Anodes for Lithiumâ€lon Batteries. ChemistrySelect, 2018, 3, 10338-10344.	0.7	28
58	HPAM–HABS induced synthesis of a labyrinth-like surface of calcite via rhombohedral lattice growth from the nanoscale. CrystEngComm, 2018, 20, 3445-3448.	1.3	5
59	Oneâ€Step Controllable Synthesis of Mesoporous MgCo ₂ O ₄ Nanosheet Arrays with Ethanol on Nickel Foam as an Advanced Electrode Material for Highâ€Performance Supercapacitors. Chemistry - A European Journal, 2018, 24, 14982-14988.	1.7	37
60	Synthesis of mesoporous orthorhombic LiMnO ₂ cathode materials via a one-step flux method for high performance lithium-ion batteries. Materials Research Express, 2018, 5, 065511.	0.8	9
61	Polymorphic Crystallization and Diversified Growth of CaCO ₃ in HPAMâ€HABSâ€Na ₂ SiO ₃ Hybrid Solutions. ChemistrySelect, 2018, 3, 6050-6055.	0.7	3
62	Electrochemiluminescence Detection of <i>Escherichia coli</i> O157:H7 Based on a Novel Polydopamine Surface Imprinted Polymer Biosensor. ACS Applied Materials & Interfaces, 2017, 9, 5430-5436.	4.0	150
63	Silver Nanoparticle Generators: Silicon Dioxide Microspheres. Chemistry - A European Journal, 2017, 23, 6244-6248.	1.7	7
64	Influence of thermal temperature on the structure and sealed micropores of stabilized polyacrylonitrile fibers. Chemical Research in Chinese Universities, 2017, 33, 312-317.	1.3	5
65	The synthesis and magnetic properties of BaFe2Se3 single crystals. RSC Advances, 2017, 7, 30433-30438.	1.7	9
66	Preparation of CdTe nanocrystals doped fluorescent silica spheres by sol-gel method and their surface modification via thiol-ene chemistry. Chemical Research in Chinese Universities, 2017, 33, 327-332.	1.3	1
67	CO.5 PAMAM dendrimers improve the kinetic stabilization and nanoscale precipitation mechanism of amorphous calcium carbonate. RSC Advances, 2017, 7, 45113-45120.	1.7	2
68	Heterostructural MnO ₂ @NiS ₂ /Ni(OH) ₂ materials for high-performance pseudocapacitor electrodes. RSC Advances, 2017, 7, 44289-44295.	1.7	26
69	Patterns of Clay Minerals Transformation in Clay Gouge, with Examples from Revers Fault Rocks in Devonina Niqiuhe Formation in The Dayangshu Basin. Acta Geologica Sinica, 2017, 91, 59-60.	0.8	0
70	High-pressure synthesis, crystal structure and photoluminescence properties of a new terbium silicate: Na ₂ Tb _{1.08} Ca _{2.92} Si ₆ O ₁₈ H _{0.8} . RSC Advances, 2017, 7, 50195-50199.	1.7	3
71	Microwave-assisted synthesis of novel nanostructured Zn ₃ (OH) ₂ V ₂ O ₇ ·2H ₂ O and Zn ₂ V ₂ O ₇ as electrode materials for supercapacitors. New Journal of Chemistry, 2017, 41, 15298-15304.	1.4	39
72	Microwave synthesis and photocatalytic activity of Tb 3+ doped BiVO 4 microcrystals. Journal of Colloid and Interface Science, 2016, 483, 307-313.	5.0	29

#	Article	IF	CITATIONS
73	Fabrication of porous double-urchin-like MgCo2O4 hierarchical architectures for high-rate supercapacitors. Journal of Alloys and Compounds, 2016, 688, 933-938.	2.8	54
74	Fabrication of a Stainlessâ€Steelâ€Meshâ€Supported Hierarchical Fe ₂ O ₃ @NiCo ₂ O ₄ Coreâ€Shell Tubular Array Anode for Lithiumâ€Ion Battery. ChemistrySelect, 2016, 1, 5569-5573.	0.7	20
75	Facile synthesis of hierarchical CoMoO ₄ @NiMoO ₄ core–shell nanosheet arrays on nickel foam as an advanced electrode for asymmetric supercapacitors. Journal of Materials Chemistry A, 2016, 4, 18578-18584.	5.2	171
76	β-NaYF4:Yb,Tm: upconversion properties by controlling the transition probabilities at the same energy level. Inorganic Chemistry Frontiers, 2016, 3, 1082-1090.	3.0	9
77	Synthesis of LiMn2O4 nano-wires via flux method and their usage as cathode material for lithium ion batteries. Chemical Research in Chinese Universities, 2015, 31, 820-824.	1.3	2
78	Synthesis of perovskite-type manganites Yb _{1â^'x} Dy _x MnO ₃ (0.1 ≤ â‰ and magnetic property studies. New Journal of Chemistry, 2015, 39, 2596-2601.	₽Tj ETQq0 1.4	0 0 rgBT /0 8
79	Spin rotation driven ferroelectric polarization with a 180° flop in double-perovskite Lu2CoMnO6. RSC Advances, 2015, 5, 43432-43439.	1.7	8
80	Alpha-Oxo Acids Assisted Transformation of FeS to Fe ₃ S ₄ at Low Temperature: Implications for Abiotic, Biotic, and Prebiotic Mineralization. Astrobiology, 2015, 15, 1043-1051.	1.5	14
81	Facile Synthesis of Three Dimensional NiCo2O4@MnO2 Core–Shell Nanosheet Arrays and its Supercapacitive Performance. Electrochimica Acta, 2015, 157, 31-40.	2.6	88
82	Nickel foam supported mesoporous NiCo ₂ O ₄ arrays with excellent methanol electro-oxidation performance. New Journal of Chemistry, 2015, 39, 6491-6497.	1.4	61
83	Rapid microwave-assisted hydrothermal synthesis of SrWO4:Eu3+ nanowires and their luminescence properties. Chemical Research in Chinese Universities, 2015, 31, 175-178.	1.3	1
84	Synthesis, crystal structure, and luminescence properties of a new microporous europium silicate: Na3EuSi6O15·1.47H2O. RSC Advances, 2015, 5, 29121-29125.	1.7	5
85	Full and ideal mixing behavior between Zr–Wd (K2ZrSi3O9) and Ti–Wd (K2TiSi3O9): evidences from mineral chemistry, X-ray diffraction pattern and Raman spectrum. Physics and Chemistry of Minerals, 2015, 42, 223-234.	0.3	7
86	Synthesis and characterization of multipod frameworks of Cu ₂ 0 microcrystals and Cu ₇ S ₄ hollow microcages. CrystEngComm, 2015, 17, 3908-3911.	1.3	10
87	Negative magnetism in perovskite manganites Gd1-x Sr x MnO3(0.1≤â‰0.3). Chemical Research in Chinese Universities, 2015, 31, 699-703.	1.3	13
88	Liquid-phase exfoliation of graphene in organic solvents with addition of naphthalene. Journal of Colloid and Interface Science, 2014, 418, 37-42.	5.0	76
89	Morphology-controlled synthesis and growth mechanisms of branched α-MnO2 nanorods via facile microwave-assisted hydrothermal method. Journal of Materials Science: Materials in Electronics, 2014, 25, 906-913.	1.1	7
90	Facile microwave-assisted synthesis and effective photocatalytic hydrogen generation of Zn ₂ GeO ₄ with different morphology. RSC Advances, 2014, 4, 15048-15054.	1.7	19

#	Article	IF	CITATIONS
91	Selective synthesis of cubic and hexagonal phase of CuInS ₂ nanocrystals by microwave irradiation. RSC Advances, 2014, 4, 16022.	1.7	16
92	High pressure synthesis, structure, and multiferroic properties of two perovskite compounds Y ₂ FeMnO ₆ and Y ₂ CrMnO ₆ . Dalton Transactions, 2014, 43, 1691-1698.	1.6	44
93	Microwave-assisted synthesis of Cu ₂ O microcrystals with systematic shape evolution from octahedral to cubic and their comparative photocatalytic activities. RSC Advances, 2014, 4, 38059-38063.	1.7	17
94	A facile template-free approach for the solid-phase synthesis of CoS ₂ nanocrystals and their enhanced storage energy in supercapacitors. RSC Advances, 2014, 4, 50220-50225.	1.7	60
95	One-step synthesis of hierarchical ZnCo ₂ O ₄ @ZnCo ₂ O ₄ core–shell nanosheet arrays on nickel foam for electrochemical capacitors. RSC Advances, 2014, 4, 38073.	1.7	24
96	High-temperature, high-pressure hydrothermal synthesis, crystal structure and photoluminescent properties, of K3[Gd1â~xTbxGe3O8(OH)2] (x = 0, 0.3, 0.1, 1). RSC Advances, 2014, 4, 26951-26955.	1.7	10
97	Hydrothermal approach and luminescent properties for the synthesis of orthoniobates GdNbO ₄ :Ln ³⁺ (Ln = Dy, Eu) single crystals under high-temperature high-pressure conditions. New Journal of Chemistry, 2014, 38, 4249-4257.	1.4	34
98	Rapid microwave synthesis of δ-MnO2 microspheres and their electrochemical property. Journal of Materials Science: Materials in Electronics, 2013, 24, 2189-2196.	1.1	13
99	Expansivity and compressibility of strontium fluorapatite and barium fluorapatite determined by in situ X-ray diffraction at high-T/P conditions: significance of the M-site cations. Physics and Chemistry of Minerals, 2013, 40, 349-360.	0.3	13
100	High pressure flux synthesis of LaMnO3+l̂´ with charge ordering. RSC Advances, 2013, 3, 21311.	1.7	3
101	Rapid microwave-assisted hydrothermal synthesis of morphology-tuned MnO2 nanocrystals and their electrocatalytic activities for oxygen reduction. Materials Research Bulletin, 2013, 48, 2696-2701.	2.7	25
102	Reversible transformation between α-oxo acids and α-amino acids on ZnS particles: a photochemical model for tuning the prebiotic redox homoeostasis. International Journal of Astrobiology, 2013, 12, 69-77.	0.9	8
103	Direct microwave-assisted amino acid synthesis by reaction of succinic acid and ammonia in the presence of magnetite. International Journal of Astrobiology, 2013, 12, 331-336.	0.9	4
104	Controlled growth of mesoporous ZnCo ₂ O ₄ nanosheet arrays on Ni foam as high-rate electrodes for supercapacitors. RSC Advances, 2013, 4, 2393-2397.	1.7	85
105	Selfâ€Assembled NaY(WO ₄) ₂ Hierarchical Dumbbells: Microwaveâ€Assisted Hydrothermal Synthesis and Their Tunable Upconversion Luminescent Properties. European Journal of Inorganic Chemistry, 2012, 2012, 2220-2225.	1.0	13
106	Microwave synthesis of NaLa(MoO4)2 microcrystals and their near-infrared luminescent properties with lanthanide ion doping (Er3+, Nd3+, Yb3+). Inorganic Chemistry Communication, 2011, 14, 1723-1727.	1.8	55
107	One-step green synthesis of cuprous oxide crystals with truncated octahedra shapes via a high pressure flux approach. Journal of Solid State Chemistry, 2011, 184, 2097-2102.	1.4	18
108	Orientation of channel carbonate ions in apatite: Effect of pressure and composition. American Mineralogist, 2011, 96, 1148-1157.	0.9	35

#	Article	IF	CITATIONS
109	Large reversible magnetocaloric effect in HoTiO3 single crystal. Journal of Applied Physics, 2011, 110, 083912.	1.1	18
110	Enhanced high temperature thermoelectric characteristics of transition metals doped Ca3Co4O9+l̂´ by cold high-pressure fabrication. Journal of Applied Physics, 2010, 107, .	1.1	102
111	New Lanthanide Silicates Based on Anionic Silicate Chain, Layer, and Framework Prepared under High-Temperature and High-Pressure Conditions. Inorganic Chemistry, 2010, 49, 9833-9838.	1.9	28
112	Correlation of structural distortion with magnetic properties in electron-doped Ca0.9R0.1MnO3 perovskites (R=rare-earth). Journal of Applied Physics, 2010, 108, 063928.	1.1	11
113	Helical chain observed under transmission electron microscope: Synthesis and structure refinement of lutetium disilicate Lu2Si2O7. CrystEngComm, 2010, 12, 1617.	1.3	11
114	High Temperature Thermoelectric Response of Electron-Doped CaMnO ₃ . Chemistry of Materials, 2009, 21, 4653-4660.	3.2	149
115	Calcium L2,3-edge XANES of carbonates, carbonate apatite, and oldhamite (CaS). American Mineralogist, 2009, 94, 1235-1241.	0.9	55
116	Selective Synthesis and Formation Mechanism of TiS ₂ Dendritic Crystals. Crystal Growth and Design, 2008, 8, 4460-4464.	1.4	22
117	Phosphane and Phosphite Unsymmetrically Disubstituted Diiron Complexes Related to the Fe-Only Hydrogenase Active Site. European Journal of Inorganic Chemistry, 2007, 2007, 3718-3727.	1.0	32
118	High-pressure synthesis and single-crystal structure refinement of gadolinium holmium silicate hydroxyapatite Gd4.33Ho4.33(SiO4)6(OH)2. Journal of Solid State Chemistry, 2006, 179, 2245-2250.	1.4	11
119	Bundle of Nanobelts Up to 4 cm in Length: One-Step Synthesis and Preparation of Titanium Trisulfide (TiS3) Nanomaterials. European Journal of Inorganic Chemistry, 2006, 2006, 519-522.	1.0	16
120	Influence of Tertiary Phosphanes on the Coordination Configurations and Electrochemical Properties of Iron Hydrogenase Model Complexes: Crystal Structures of [(μ-S2C3H6)Fe2(CO)6-nLn] (L =) Tj ETQ	∑գ Ω ወՕrgI	BT1 #0 verlock
121	Preparation and luminescence properties investigation of Eu3+, Tb3+-doped LaNbO4:RE3+ (RE = Eu, Eu/	Tb,) Tj ET(1.1	Չգ <u>1</u> 1 0.784

¹²² Two-in-one template-assisted construction of hollow phosphide nanotubes for electrochemical energy storage. Inorganic Chemistry Frontiers, 0, , .

3.0 1